ChemComm

COMMUNICATION

View Article Online
View Journal | View Issue

Cite this: *Chem. Commun.*, 2023, 59, 1777

Received 9th December 2022,
Accepted 17th January 2023

DOI: 10.1039/d2cc06730g

rsc.li/chemcomm

Lignin C–C bond cleavage induced by consecutive two-photon excitation of a metal-free photocatalyst†

Pengju Li, Rong Liu, Zijian Zhao, Fushuang Niu and Ke Hu *

Photocatalytic lignin valorization has caught widespread attention; yet the reaction systems often employ noble metal complexes, hydrogen atom transfer (HAT) agents, and/or sacrificial electron donors/acceptors that do not comply with atom economy or environmental friendliness. Herein, we discovered that *N*-phenylphenothiazine (PTH) as a metal-free photocatalyst induced the cleavage of the lignin C_α–C_β bond under ambient conditions free of those additional agents with a high yield and selectivity toward benzoic acid. Transient spectroscopic investigations revealed that the energy-demanding C_α–C_β bond cleavage was induced by the potent oxidant, $^2PTH^{\bullet+}$*, that was derived from consecutive two-photon excitation of PTH.

Lignin, rich in aromatic carbon units, is a renewable energy source to replace the use of fossil fuels on a large scale. Yet breaking the profuse C–O and C–C bonds selectively into small value-added compounds is challenging. Currently, various strategies have been reported for the valorization of lignin, including pyrolysis, gasification, acid or base treatment, hydrogenolysis, *etc.*[1–5] These methods often require harsh reaction conditions such as high temperature, high pressure, corrosive solvents, *etc.*, so better methods are urgently needed. Photocatalysis, typically considered as a green and mild method for organic redox synthesis, has gained increasing popularity for biomass valorization.[6–14] However, cleavage of the high energy C–C or C–O bonds requires potent photooxidants or photoreductants, among which noble-metal-containing ruthenium or iridium coordination compounds are often used.[15–19] Furthermore, hydrogen atom transfer (HAT) agents and sacrificial electron or hole donors are often used as necessary additives in an inert atmosphere to complete the catalytic cycle.[15,16,18,20–25] These additives generate unproductive waste to the extent that the value of the obtained small aromatic compounds may not offset it. Therefore, it is highly desirable to find a photocatalytic strategy that can selectively cleave lignin C–C bonds into high-value-added aromatic compounds in an ambient environment without metal-containing photocatalysts, sacrificial reagents or other additives.

Herein, we report that *N*-phenylphenothiazine (PTH) as a metal-free photocatalyst surprisingly induces the selective cleavage of lignin C_α–C_β bonds under ambient conditions without any other additives. Though a mild photooxidant in its singlet excited state, the doublet excited state of the radical cation ($^2PTH^{\bullet+}$*) is a potent photooxidant to induce the oxidative cleavage of the C_α–C_β bond in lignin models through consecutive two-photon excitation (Scheme 1). Two-color two-pulse laser flash photolysis experiments revealed a rapid subnanosecond electron transfer process likely through a static quenching mechanism.[26–28] A wide scope of major lignin units were successfully cleaved in high yields through simple steady state illumination of PTH, demonstrating the potential utility of this simple, commercially-available, metal-free photocatalyst for lignin valorization in an environmentally-friendly manner.

PTH showed mainly UV absorption in the ground state (Fig. 1a). Electrochemical oxidation of PTH in CH_3CN resulted in $PTH^{\bullet+}$ formation showing three distinctive visible to near IR absorption bands (λ_{max} = 514 nm, 772 nm, and 864 nm) (Fig. S1, ESI†) that were consistent with the literature.[29] $PTH^{\bullet+}$ was air-stable as the absorption was retained upon solution exposure to the air. When the PTH solution was irradiated with 390 nm light in ambient air, a similar absorption change attributed to the formation of $PTH^{\bullet+}$ was also observed (Fig. S2, ESI†). Molecular oxygen dissolved in CH_3CN

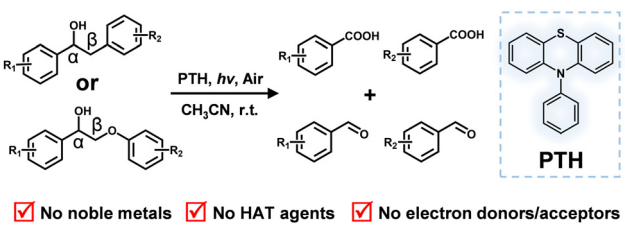

Scheme 1 Photocatalytic cleavage of the C_α–C_β bond of lignin model substrates.

Department of Chemistry and Shanghai Key Laboratory of Molecular Catalysis and Innovative Materials, Fudan University, 220 Handan Road, Shanghai 200433, P. R. China. E-mail: khu@fudan.edu.cn

† Electronic supplementary information (ESI) available. See DOI: https://doi.org/10.1039/d2cc06730g

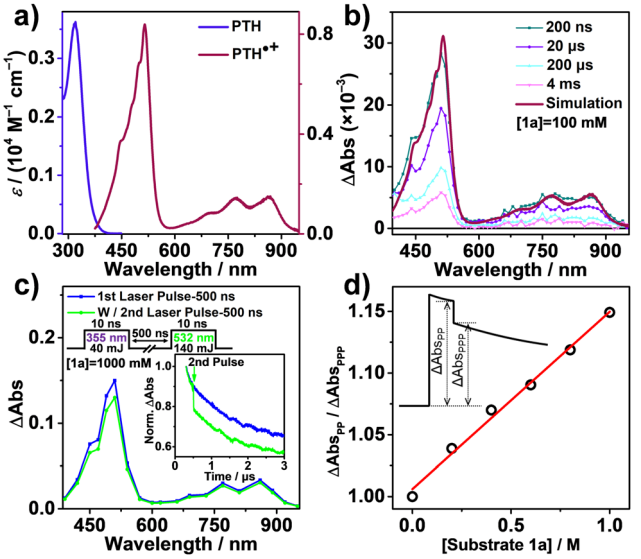

Fig. 1 (a) The UV-vis-NIR absorption spectra of PTH and PTH$^{\bullet+}$ in CH_3CN. (b) Full TA spectra of PTH obtained after 355 nm pulsed-laser excitation in the presence of 100 mM **1a** in aerated CH_3CN at the indicated time delays. (c) Absorption difference spectra of PTH in the presence of 1000 mM **1a** in a two-color two-pulse TA experiment at 500 ns time delay before the second laser pulse (blue) and after the second laser pulse (green). Inset: Transient kinetic data monitored at the probe wavelength of 510 nm for PTH$^{\bullet+}$ with a two-color two-pulse laser excitation sequence shown in the laser pulse scheme above (kinetics in green) or with only the first 355 nm pulsed-laser excitation (kinetics in blue). (d) Stern–Volmer-type plot based on the two-color two-pulse TA experiment at different concentrations of **1a**. The subscript PP stands for pump-probe and PPP pump–pump–probe. The inset shows the meaning of ΔAbs_{PP} and ΔAbs_{PPP}.

was presumably the electron acceptor responsible for quenching the PTH excited state (Fig. S3, ESI†).[30]

Cyclic voltammetry (CV) was performed to evaluate the redox properties of PTH and the lignin model substrate 1,2-diphenylethanol (**1a**). PTH showed a reversible redox wave at $E^{\circ}(PTH^{\bullet+/0}) = 0.92$ V *vs.* NHE (Fig. S4, ESI†) and an irreversible peak at $E_{p/2} = 1.59$ V attributed to $PTH^{2+/\bullet+}$. The oxidation of **1a** was also irreversible with $E_{p/2} = 1.9$ V, which was more positive than $E_{p/2}(PTH^{2+/\bullet+})$. CV of the PTH and **1a** mixture did not show any catalytic current for the oxidation of **1a** as expected due to unfavourable thermodynamics (Fig. S4, ESI†).

A steady-state fluorescence quenching experiment was carried out to test whether the PTH excited state could oxidize **1a**. Unsurprisingly, titration of **1a** up to 100 mM did not lead to any measurable PTH fluorescent quenching (Fig. S5, ESI†). The excited state of PTH apparently lacked the oxidative power to initiate the oxidation of **1a**.

Nanosecond transient absorption (TA) spectroscopy was employed to explore the electron transfer dynamics between PTH and **1a**. Fig. 1b shows the full TA spectra of PTH in the presence of **1a** in aerated CH_3CN after nanosecond pulsed-laser excitation (λ_{ex} = 355 nm). The positive absorption bands from the visible to near infrared region corresponded to the absorption of PTH$^{\bullet+}$, which was consistent with the oxidation of PTH from both the spectroelectrochemistry and photolysis data (Fig. S2 and S6, ESI†).

The visible to NIR absorption of PTH$^{\bullet+}$ allowed it to absorb a second photon to reach the doublet excited state, PTH$^{\bullet+}$*. Prior studies have shown that PTH$^{\bullet+}$* is a potent photooxidant with $E^{\circ}(PTH^{\bullet+}*/^{0}) = 2.31$ V.[27] It was of great interest to study the PTH$^{\bullet+}$* reactivity towards the degradation of lignin models with redox potential around 2.0 V. Nanosecond two-color two-pulse TA experiments were carried out to investigate the quenching of PTH$^{\bullet+}$* by **1a**. The first laser pulse (λ_{ex} = 355 nm) generated PTH* that subsequently transferred an electron to O_2 to form the long-lived PTH$^{\bullet+}$ as the spectral simulation showed in Fig. 1b. The second laser pulse (λ_{ex} = 532 nm) was delayed by 500 ns relative to the first and selectively excited the transiently formed PTH$^{\bullet+}$. The second laser pulse resulted in significant bleaching of the PTH$^{\bullet+}$ absorption signal monitored at 510 nm in the presence of 1000 mM **1a** (Fig. 1c inset). Absorption difference spectra of PTH recorded from 390 nm – 950 nm in oxygen-saturated CH_3CN after two pulsed-laser excitations are displayed in Fig. 1c. Upon titration of increasing concentrations of **1a**, the bleach signal of delta absorbance monitored at 510 nm gradually increased right after the second laser pulse excitation. For the control sample that was in the absence of **1a**, the second laser pulse did not result in the bleaching of the PTH$^{\bullet+}$ absorption (Fig. S7, ESI†). A Stern–Volmer-type plot for the quenching of PTH$^{\bullet+}$* by **1a** was obtained by plotting $\Delta Abs_{PP}/\Delta Abs_{PPP}$ as a function of increasing concentrations of **1a** (Fig. 1d). The plot showed a linear regression, from which the slope was equal to 0.15 M^{-1}. Considering that the lifetime of PTH$^{\bullet+}$* was only 36 ps,[29] it was highly unlikely that the reductive quenching approached through bimolecular diffusion, but rather ground state association of PTH$^{\bullet+}$* and **1a** with the equilibrium constant of 0.15 M^{-1}.

Steady-state photolysis of PTH and **1a** was carried out in CH_3CN under ambient air conditions. Deviations from the standard condition along with the reaction conversions and product yields are also listed in Table 1. First, we optimized the photocatalyst PTH concentration and chose 15 mol% as the standard reaction concentration since concentration as high as 20 mol% did not result in a significant increase in the product yield (Table 1, entries 1–3). Three major products were detected including benzoic acid (**1b**), benzaldehyde (**1c**), and diphenylethanone (**1d**). The formation of **1b** and **1c** clearly demonstrated that PTH under light promoted oxidative cleavage of the C_α–C_β bond in appreciable yields (entry 1). Note that 100% selective C_α–C_β bond cleavage in **1a** would theoretically result in 200% yield of **1b** and **1c** combined. Nevertheless, the combined yield of 96% was still among the average of lignin C_α–C_β bond cleavage in the literature;[18,31] yet our photocatalytic system only contained PTH photocatalyst without other HAT or sacrificial agents. It is also noteworthy that when a white light LED source was added in combination with the 390 nm light, the rate of product formation was significantly faster than using 390 nm light irradiation alone (Fig. S8, ESI†). Greater visible light absorption by PTH$^{\bullet+}$ was indeed helpful for the generation of PTH$^{\bullet+}$*.

When the ambient air environment was replaced by Ar, there was almost no conversion of **1a** and no product was detected (entry 4). The solution dissolved molecular oxygen was

Table 1 Reaction Optimization for the Steady-State Photolysis of the Lignin Model **1a**

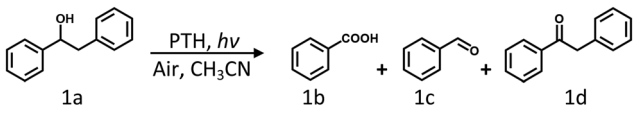

Entry	Deviation from standard conditions	Con. (%)	Yield of products (%) 1b	1c	1d
1	None	96	82	14	23
2	10 mol% PTH	93	66	16	24
3	20 mol% PTH	96	87	16	24
4	Ar instead of air	n.r.	n.d	n.d.	n.d.
5	In the dark	n.r.	n.d	n.d.	n.d.
6	No PTH	33	12	8	12
7	2,6-Lutidine (4 equiv.)	30	5	1	5
8	HCOOH (4 equiv.)	85	43	18	22
9	10% water	76	31	16	28
10	$AgNO_3$	71	27	11	39
11	BQ	66	11	18	36
12	TEOA	24	1	1	1
13	TEMPO	25	1	3	1
14	MeOH instead of CH_3CN	36	5	3	12

Standard reaction conditions: 0.1 mmol **1a**, 15 mol% PTH, 2 mL CH_3CN, 390 nm LED (15 mW·cm^{-2}), air, 48 h, room temperature. Yield of **1b**, **1c**, **1d** = moles of product **1b**, **1c**, **1d** formed/moles of **1a** × 100%. n.r. = no reaction. n.d. = not detected. All yields were determined by HPLC analysis. Electron, hole, or radical scavengers: 200 mM $AgNO_3$, 200 mM BQ, 200 mM TEOA, 200 mM TEMPO.

the default electron acceptor for PTH*, while PTH* by itself was unable to perform photoredox chemistry towards **1a** as suggested by the previous fluorescence quenching experiment. When the reaction was placed in the dark, no conversion of **1a** was found, which eliminated the possibility of thermoreactions (entry 5). Conversion of **1a** in the absence of PTH was observed but in a much slower rate (entry 6). The observation was not unprecedented though when lignin substrates were exposed to UV light.[32,33] The above variations of reaction conditions confirmed that light, photocatalyst, and O_2 were all essential factors to achieve efficient C_α–C_β bond cleavage for **1a**. It is noteworthy that the addition of other environmental factors such as acid, base, or water dramatically suppressed the yields of C_α–C_β bond cleavage products (entries 7–9). As we emphasized, the PTH photocatalyzed C_α–C_β bond cleavage for **1a** proceeded under mild conditions without the need for additional additives.

The scope of the lignin model substrates that included β–1 and β–O–4 linkages (2a–6a) was also investigated for PTH photocatalyzed C_α–C_β bond cleavage reactions. The oxidations of 2a–6a were all irreversible with $E_{p/2}$ spanning between 1.59 V and 1.92 V (Fig. S9–S13, ESI†), which were well below $E^\circ(PTH^{\bullet+*/0})$. The photocatalytic reaction conversions were all close to 100% across the substrate scope under the standard reaction conditions (Table S1, ESI†). Substituents to the aromatic rings of **1a** resulted in comparatively high yields and selectivity as well (Table S1, entries 2 and 3, ESI†). Similar to the β–1 model, the C_α–C_β bond of the β–O–4 linkage model was also cleaved with moderate yields under the standard reaction conditions (Table S1, entries 4 and 5, ESI†).

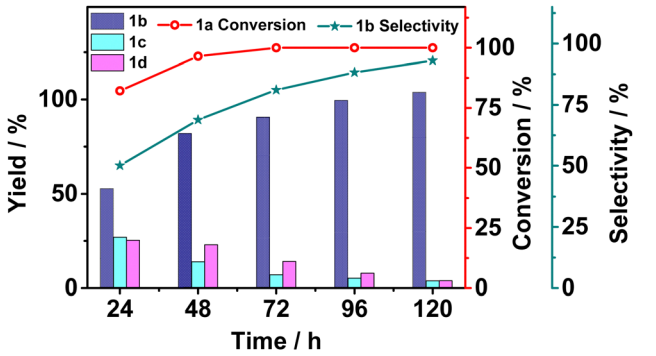

Fig. 2 The product yields from photocatalytic C_α–C_β bond cleavage of **1a** over the elapsed time. **1b** selectivity = moles of product **1b**/moles of product (**1b** + **1c** + **1d**) × 100%.

Although **1a** conversion approached unity after 48 hours of photocatalysis, the uncleaved product **1d** was still present in a significant amount. Therefore, we set out to monitor the product yields by sampling the reaction solution every 24 hours (Fig. 2). The conversion of **1a** climbed close to unity within 48 hours and stayed almost invariant in the next 120 hours, but the ratio of the product yields kept changing over time. Initially, all three products were present but the yields of **1c** and the uncleaved product **1d** gradually decreased to almost 0 while that of **1b** increased to almost the only product. The yields of products over time suggested that **1d** might be the kinetically competitive product but was subject to further photoredox induced cleavage to the final thermodynamically stable **1b**. The long-time photolysis result was encouraging in terms of selectively obtaining high purity of the C_α–C_β-bond-cleaved photoproduct.

Electron, hole, and radical scavengers including $AgNO_3$, 1, 4-benzoquinone (BQ), triethanolamine (TEOA), and 2,2,6, 6-tetramethylpiperidine-1-oxyl (TEMPO) were used to test possible reactive intermediates for elucidation of the reaction mechanism (Table 1, entries 10–13). The addition of TEOA significantly decreased the product yields, suggesting that $PTH^{\bullet+*}$ was a necessity. The formation of $O_2^{\bullet-}$ was also critical to the reaction conversion because BQ as a superoxide scavenger and $AgNO_3$ as a competitive electron acceptor to O_2 could both significantly decrease the product yields. The addition of TEMPO dramatically reduced the efficiency of the reaction, indicating that the catalytic process involved free radical intermediates.

Based on the above control tests and transient spectroscopic data, the following photocatalytic mechanism was proposed for lignin C_α–C_β bond cleavage (Scheme 2). Under the first photon irradiation, the photoexcited PTH was oxidatively quenched by O_2 with $PTH^{\bullet+}$ and $O_2^{\bullet-}$ as the primary photoproducts. $PTH^{\bullet+}$ was insufficient to oxidize **1a**, but with its absorption of the second photon, the doublet excited state $PTH^{\bullet+*}$ was a superoxidant ($E^\circ(PTH^{\bullet+*/0}) > 2.3$ V) that abstracted an electron to generate a C_β-centered radical and released a proton (H^+). Subsequently, the C_β-centered radical of **1a** reacted with $O_2^{\bullet-}$ and H^+ to produce a peroxide intermediate. Next, the unstable

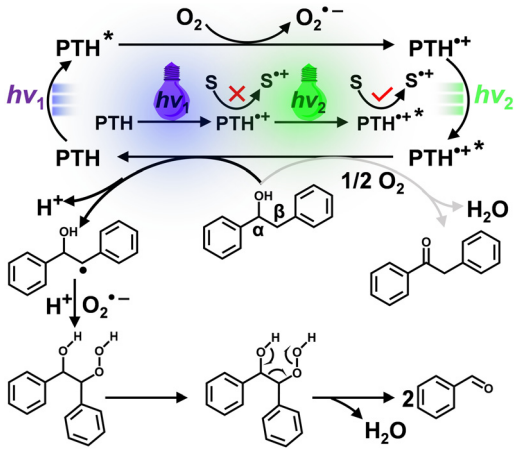

Scheme 2 Proposed mechanism for C_α–C_β bond cleavage of **1a** *via* consecutive photo-excitation of the PTH photocatalyst.

peroxide intermediate induced cleavage of the C_α–C_β bond to form benzaldehyde and water.[34] Control experiments showed that benzaldehyde was further oxidized to produce benzoic acid.

In summary, we proposed a new photocatalytic strategy where a commercially available, metal-free small organic photocatalyst, PTH, can be used to valorize lignin under ambient air conditions through photocatalysis. The doublet excited state $PTH^{\bullet+}*$ formed from consecutive two-photon excitation was a potent oxidant to activate the $C(sp^3)$–H bond of lignin models possibly through ground state association with the substrate and subsequently induced C_α–C_β bond cleavage. The conversion of a variety of major lignin models was close to unity with a benzoic acid moiety as the major photocleaved product. The reaction conditions were mild without any additional HAT agents and sacrificial electron/hole donors. Therefore, the photocatalytic strategy is a green approach to value-added carbon sources from lignin waste.

This work is supported by the National Natural Science Foundation of China (22173022) and the Natural Science Foundation of Shanghai (21ZR1404400, 19DZ2270100).

Conflicts of interest

There are no conflicts to declare.

Notes and references

1 Y. Liao, S.-F. Koelewijn, G. Van den Bossche, J. Van Aelst, S. Van den Bosch, T. Renders, K. Navare, T. Nicolaï, K. Van Aelst and M. Maesen, *Science*, 2020, **367**, 1385–1390.
2 W.-J. Liu, W.-W. Li, H. Jiang and H.-Q. Yu, *Chem. Rev.*, 2017, **117**, 6367–6398.
3 C. Li, X. Zhao, A. Wang, G. W. Huber and T. Zhang, *Chem. Rev.*, 2015, **115**, 11559–11624.
4 Q. Meng, J. Yan, R. Wu, H. Liu, Y. Sun, N. Wu, J. Xiang, L. Zheng, J. Zhang and B. Han, *Nat. Commun.*, 2021, **12**, 1–12.
5 Z. Liu, H. Li, X. Gao, X. Guo, S. Wang, Y. Fang and G. Song, *Nat. Commun.*, 2022, **13**, 1–11.
6 X. Wu, X. Fan, S. Xie, J. Lin, J. Cheng, Q. Zhang, L. Chen and Y. Wang, *Nat. Catal.*, 2018, **1**, 772–780.
7 N. Luo, T. Montini, J. Zhang, P. Fornasiero, E. Fonda, T. Hou, W. Nie, J. Lu, J. Liu and M. Heggen, *Nat. Energy*, 2019, **4**, 575–584.
8 H. Liu, H. Li, J. Lu, S. Zeng, M. Wang, N. Luo, S. Xu and F. Wang, *ACS Catal.*, 2018, **8**, 4761–4771.
9 X. Wu, S. Xie, C. Liu, C. Zhou, J. Lin, J. Kang, Q. Zhang, Z. Wang and Y. Wang, *ACS Catal.*, 2019, **9**, 8443–8451.
10 G. Han, T. Yan, W. Zhang, Y. C. Zhang, D. Y. Lee, Z. Cao and Y. Sun, *ACS Catal.*, 2019, **9**, 11341–11349.
11 X. Wu, N. Luo, S. Xie, H. Zhang, Q. Zhang, F. Wang and Y. Wang, *Chem. Soc. Rev.*, 2020, **49**, 6198–6223.
12 S.-H. Li, S. Liu, J. C. Colmenares and Y.-J. Xu, *Green Chem.*, 2016, **18**, 594–607.
13 M.-Y. Qi, M. Conte, M. Anpo, Z.-R. Tang and Y.-J. Xu, *Chem. Rev.*, 2021, **121**, 13051–13085.
14 M.-Y. Qi, M. Conte, Z.-R. Tang and Y.-J. Xu, *ACS Nano*, 2022, **16**, 17444–17453.
15 K. Chen, J. Schwarz, T. A. Karl, A. Chatterjee and B. König, *Chem. Commun.*, 2019, **55**, 13144–13147.
16 G. Magallanes, M. D. Karkas, I. Bosque, S. Lee, S. Maldonado and C. R. Stephenson, *ACS Catal.*, 2019, **9**, 2252–2260.
17 Q. Zhu and D. G. Nocera, *ACS Catal.*, 2021, **11**, 14181–14187.
18 E. Ota, H. Wang, N. L. Frye and R. R. Knowles, *J. Am. Chem. Soc.*, 2019, **141**, 1457–1462.
19 S. Li, S. Kim, A. H. Davis, J. Zhuang, E. W. Shuler, D. Willinger, J.-J. Lee, W. Zheng, B. D. Sherman and C. G. Yoo, *ACS Catal.*, 2021, **11**, 3771–3781.
20 I. Bosque, G. Magallanes, M. Rigoulet, M. D. Kärkäs and C. R. Stephenson, *ACS Cent. Sci.*, 2017, **3**, 621–628.
21 S. T. Nguyen, P. R. Murray and R. R. Knowles, *ACS Catal.*, 2019, **10**, 800–805.
22 J. D. Nguyen, B. S. Matsuura and C. R. Stephenson, *J. Am. Chem. Soc.*, 2014, **136**, 1218–1221.
23 C. Yang, M. D. Karkas, G. Magallanes, K. Chan and C. R. Stephenson, *Org. Lett.*, 2020, **22**, 8082–8085.
24 H. Li and O. S. Wenger, *Angew. Chem., Int. Ed.*, 2022, **61**, e202110491.
25 S. Li, Z. Hao, K. Wang, M. Tong, Y. Yang, H. Jiang, Y. Xiao and F. Zhang, *Chem. Commun.*, 2020, **56**, 11243–11246.
26 F. Glaser and O. S. Wenger, *JACS Au*, 2022, **2**, 1488–1503.
27 P. Li, A. M. Deetz, J. Hu, G. J. Meyer and K. Hu, *J. Am. Chem. Soc.*, 2022, **144**, 17604–17610.
28 S. Wu, J. Žurauskas, M. Domański, P. S. Hitzfeld, V. Butera, D. J. Scott, J. Rehbein, A. Kumar, E. Thyrhaug and J. Hauer, *Org. Chem. Front.*, 2021, **8**, 1132–1142.
29 J. A. Christensen, B. T. Phelan, S. Chaudhuri, A. Acharya, V. S. Batista and M. R. Wasielewski, *J. Am. Chem. Soc.*, 2018, **140**, 5290–5299.
30 S. Alkaitis, G. Beck and M. Grätzel, *J. Am. Chem. Soc.*, 1975, **97**, 5723–5729.
31 Y. Wang, Y. Liu, J. He and Y. Zhang, *Sci. Bull.*, 2019, **64**, 1658–1666.
32 Y. Kang, X. Yao, Y. Yang, J. Xu, J. Xin, Q. Zhou, M. Li, X. Lu and S. Zhang, *Green Chem.*, 2021, **23**, 5524–5534.
33 A. Temiz, U. C. Yildiz, I. Aydin, M. Eikenes, G. Alfredsen and G. Çolakoglu, *Appl. Surf. Sci.*, 2005, **250**, 35–42.
34 T. Hou, N. Luo, H. Li, M. Heggen, J. Lu, Y. Wang and F. Wang, *ACS Catal.*, 2017, **7**, 3850–3859.

